Intra-operative Volume Imaging of the Left Atrium and Pulmonary Veins with Rotational X-Ray Angiography

Robert Manzke[1], Vivek Y. Reddy[2], Sandeep Dalal[1],
Annemarie Hanekamp[1], Volker Rasche[3], and Raymond C. Chan[1]

[1] Philips Research North America, Clinical Sites Research,
345 Scarborough Road, Briarcliff Manor, NY, USA
robert.manzke@philips.com
[2] Experimental Electrophysiology Laboratory, Cardiac Arrhythmia Service,
Massachusetts General Hospital, Boston, USA
[3] University Clinic Ulm, Germany

Abstract. Complex electrophysiology (EP) procedures, such as catheter-based ablation in the left atrium and pulmonary veins (LAPV) for treatment of atrial fibrillation, require knowledge of heart chamber anatomy. Electroanatomical mapping (EAM) is typically used to define cardiac structures by combining electromagnetic spatial catheter localization with surface models which interpolate the anatomy between EAM point locations in 3D. Recently, the incorporation of pre-operative volumetric CT or MR data sets has allowed for more detailed maps of LAPV anatomy to be used intra-operatively. Preoperative data sets are however a rough guide since they can be acquired several days to weeks prior to EP intervention. Due to positional and physiological changes, the intra-operative cardiac anatomy can be different from that depicted in the pre-operative data.

We present a novel application of contrast-enhanced rotational X-ray imaging for CT-like reconstruction of 3D LAPV anatomy during the intervention itself. We perform two selective contrast-enhanced rotational acquisitions and reconstruct CT-like volumes with 3D filtered back projection. Two volumes depicting the left and right portions of the LAPV are registered and fused. The combined data sets are then visualized and segmented intra-procedurally to provide anatomical data and surface models for intervention guidance. Our results from animal and human experiments indicate that the anatomical information from intra-operative CT-like reconstructions compares favorably with pre-acquired CT data and can be of sufficient quality for intra-operative guidance.

1 Introduction

Currently, a large number of interventional cardiac electrophysiology (EP) procedures are performed with fluoroscopic X-ray guidance alone. Two-dimensional projections from a single view are typically used to visualize catheter location and EP device placement. Minimally-invasive catheter-based ablation has become the first line therapy for many cardiac arrhythmias. However, attempts to ablate more complex arrythmia, such as atrial fibrillation (AFib), continues to be very challenging [1] because of limitations in projection imaging. Fluoroscopy times longer than one hour are not uncommon for such complex procedures, resulting in significant X-ray exposure to the patient and

R. Larsen, M. Nielsen, and J. Sporring (Eds.): MICCAI 2006, LNCS 4190, pp. 604–611, 2006.

clinical staff [2, 1]. Ablation strategies based on anatomical information from electroanatomic mapping (EAM) can improve the efficacy of catheter ablation for these complex cases [2, 1, 3], reducing the X-ray dose significantly.

EAM mapping can however be a tedious procedure which yields a sparse number of cardiac surface points through which an interpolating surface is lofted as an aid to visualization. Recently, pre-operative volumetric imaging techniques such as magnetic resonance imaging (MRI) and computed tomography (CT) have been used to provide more detailed representations of the LAPV anatomy in 3D. However, due to factors including patient positioning, volume status, and physiological variation over the often long time interval between pre-operative imaging and intervention, the anatomy from pre-operative data can be quite different from the intra-procedural heart chamber shape. MRI cannot currently be used for patients with device implants that are not MR-compatible; this clinical population represents a sizeable fraction of patients undergoing EP procedures. CT on the other hand increases the X-ray radiation exposure for the patient, beyond the dose already necessary in the intervention. Despite these limitations, the level of anatomical detail provided by pre-operative data sets has significantly improved LAPV ablation guidance when integrated intra-operatively with catheter-tracking-based EAM systems [3, 4].

To address the limitations of pre-operative imaging, we have developed a novel approach for intra-procedural 3D imaging of the LAPV anatomy. With contrast-enhanced 3D rotational X-ray angiography (3DRA) in combination with 3D filtered back projection algorithms, we are able to reconstruct the anatomy of the LA and the PVs in a CT-like fashion. We use selective contrast injections to enhance separate rotational acquisitions of the left and right portions of the LAPV structure. Following CT-like reconstruction, the two volumes are registered and fused. We then use the volumetric data intra-operatively for direct volume or cut-plane visualization and for LAPV surface segmentation.

This paper is structured as follows: Section 2 describes our methods and materials. Section 3 presents our results from CT-like 3DRA reconstruction relative to pre-operatively acquired CT data sets. Our conclusions and future work are given in section 4.

2 Methods and Materials

2.1 Clinical Imaging Protocols

3D Rotational X-Ray (3DRA). 3DRA data acquisition is performed using the Philips Allura XPer FD10 flat detector single-plane X-ray system. Two breath-hold acquisitions are performed, each with selective iodine contrast agent injection of 60cc at a rate of 20cc/s into the left/right branch of the pulmonary arteries.

The transit time of each contrast bolus through the pulmonary circulation and into the LAPV anatomy is somewhat patient-dependent and takes approximately 3-4s after initiating the injection (see Figure 1). Rotational acquisition is initiated, accounting for this delay interval, and takes 4s over which the C-arm rotates 220 degrees around the patient. 120 projections are captured at 30Hz frame rate. The overall time for each acquisition requires $\sim$10s, a very reasonable breath-hold duration.

Multislice Computed Tomography (MSCT). For comparison of 3DRA with pre-operatively acquired MSCT data sets, imaging was performed using a standard cardiac helical imaging protocol (120 kV, 500 mAs, 64×0.75mm collimation, 0.42 s rotation time) together with a conventional intravenous contrast injection protocol (20cc timing bolus, and imaging bolus of 100cc at 5cc/s). ECG-gated images were reconstructed with 0.75mm slice thickness, at 0.3mm increments, with a 20cm field-of-view, a medium smooth reconstruction filter, and a 512x512 pixel matrix.

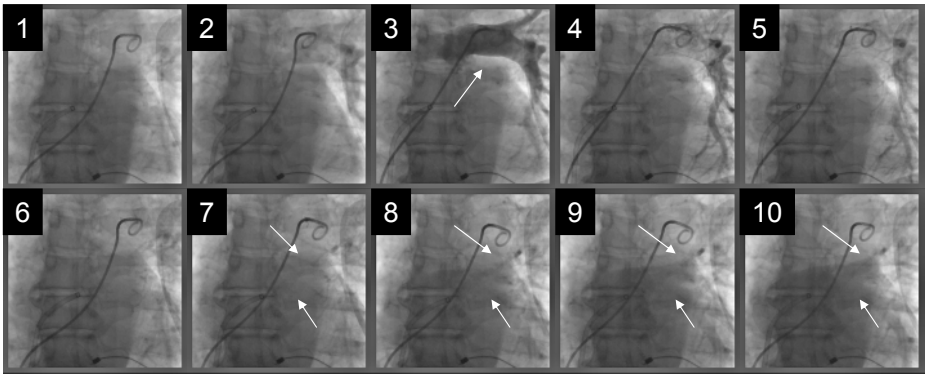

Fig. 1. Cine acquisition of a bolus injection into the left pulmonary artery (20cc at 20cc/s) where each frame corresponds to 1s. Test bolus injection takes a total of 1s and the contrast agent passes the lung in about 4s. Arrows mark opacified left PV's.

2.2 Image Reconstruction

Cone-beam projections, $p(\beta, \mu, \nu)$, from 3DRA were acquired, where β is the rotational angle, and (μ,ν) are the detector coordinates. Un-gated volume reconstruction was then performed with the standard approximate Feldkamp (FDK) cone-beam reconstruction algorithm [5], which is available on the Philips Allura platform:

$$w(\mu, \nu) = \frac{\overline{SO}}{\sqrt{\overline{SO}^2 + \mu^2 + \nu^2}}\,, \tag{1}$$

$$p^f(\beta, \mu, \nu) = \{w(\mu, \nu) \cdot p(\beta, \mu, \nu)\} * h(\mu)\,, \tag{2}$$

$$f(\mathbf{x}) = \int_0^{2\pi} \frac{\overline{SO}^2}{U^2(x, y, \beta)} p^f(\beta, \mu(x, y, \beta), \nu(\mathbf{x}, \beta)) d\beta\,, \tag{3}$$

In these equations, the distance from source to the detector is $\overline{SO}$, $h(\cdot)$ is the ramp filter kernel, $\mathbf{x} = (x, y, z)^T$ is the voxel coordinate and $f(\cdot)$ is the object function. $w(\mu, \nu)$ specifies the cone-angle dependent pre-weighting and $U(\cdot)$ is the voxel-dependent weighting of the FDK algorithm. Geometry calibration of the X-ray system is performed prior to acquisition [6].

2.3 Registration, Fusion, and Segmentation of 3DRA-Derived Volumes

Following volumetric reconstruction of data sets from the left and right pulmonary artery injections, we registered the two volumes using the thoracic vertebrae present in both acquisitions. Slight variations in breath-holds during the acquisition were disregarded. A sub-volume of interest large enough to contain the spine in both data sets was graphically-prescribed. Starting with an initial estimate of the transformation between the left and right sub-volumes in addition to trilinear interpolation of voxel intensities, the right volume was transformed into the coordinate-space of the left volume. The resulting sub-volumes were vectorized using lexicographical-ordering and normalized. The 3D normalized correlation (Equation 4) was then computed between the data sets as follows:

$$C = \hat{I}_L^T(\mathbf{x}_L)\hat{I}_R(\mathbf{T}(\mathbf{x}_R)) \tag{4}$$

where $\hat{I}_L(\mathbf{x}_L)$ and $\hat{I}_R(\mathbf{T}(\mathbf{x}_R))$ are respectively the left and right normalized volume vectors, $\mathbf{x}_L$ designates left volume coordinates, $\mathbf{x}_R$ designates right volume coordinates, and $\mathbf{T}(\mathbf{x}_R)$ designates right volume coordinates transformed into the left volume coordinate system. The cross-correlation objective function was iteratively maximized using a constrained-search of the transformation parameter space. Afterwards, the two volumes were fused for visualization and further analysis by using the average volume intensity at each grid point in the combined data set. The mean intensities of the individual volumes, $\bar{I}_L$, and $\bar{I}_R$, were used to normalize each voxel intensity before averaging as shown in Equation 5.

$$I(\mathbf{x}) = \frac{1}{2}\left\{\frac{\bar{I}_L}{\bar{I}_R} \cdot I_R(\mathbf{x}) + I_L(\mathbf{x})\right\} \tag{5}$$

Figure 2 demonstrates a result from spine registration and fusion from a sample data set.

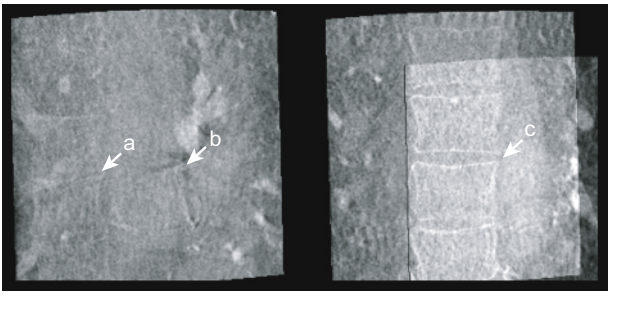

Fig. 2. Sample result to illustrate volumetric spine fusion with mis-registration on the left, and accurate registration on the right. Annotations (a) and (b) show two separate sets of spinal vertebrae due to lack of registration. Annotation (c) in the registered volume clearly shows a single vertebral column, reflecting satifactory registration.

We segmented the fused volume by graphically-specifying a seed point within the contrast-enhanced LAPV structure. With prescribed limits for the minimum and maximum voxel intensities within the LAPV, we performed threshold-based region-growing around the initial seed point to segment in 3D all connected voxels falling within the LAPV region-of-interest. Morphological erosion and dilation were used to eliminate spurious edge voxels and holes in the segmentation. A triangulated surface model was extracted from the segmented binary mask using the marching cubes isosurfacing algorithm [7] and further smoothed for comparison with models extracted from pre-operatively acquired MSCT data.

3 Results

3.1 Animal Results

Figure 3 shows volume rendered images of a reconstructed heart from porcine imaging. The procedure described in Section 2.1 was used for contrast injection, except that the contrast agent was injected into the main branch of the pulmonary artery. Due to the higher heart rate and smaller stroke volume for pigs, the contrast bolus enhanced the aorta and the left ventricle, in addition to the LAPV. The small size of the pig heart allowed for complete volume coverage in a single acquisition, obviating the need for volume registration. Good anatomical correlation between the reconstructions from 3DRA (upper row, Figure 3) and MSCT (lower row) can be appreciated. In particular, the LAPV structure is clearly identifiable within the reconstructed 3DRA data set.

3.2 Human Results

Acquisitions with selective enhancement of the left and right sides of the LAPV structure were performed (see Figure 4). Separate acquisitions were required due to field-of-view limitations of the X-ray system and rapid contrast dilution as the bolus propagates through the cardiovascular system.

A qualitative comparison of the CT-like 3DRA data relative to pre-operative CT imaging is shown in Figure 5. As it was observed for the porcine imaging study, the LAPV anatomy can clearly be appreciated. Relative to MSCT, the rotational angiography reconstructions are noisier, due to the lower angular sampling of projection data and lower detector dynamic range. The level of structural detail within the CT-like 3DRA reconstruction (top row of Figure 5) is comparable to that present within the reference MSCT volume despite the fact that reconstructions from 3DRA were performed without any cardiac gating. This finding is attributable to the low degree of LAPV motion over the cardiac cycle, especially in the presence of atrial fibrillation which disrupts the synchrony of LAPV motion.

In the last Figure 6, a segmentation surface model of the human LAPV structure is shown. Such a surface model can be used in combination with EAM to guide mapping and intervention. Segmented surfaces from 3DRA (left image) show anatomical features within the LAPV that are similar to those present in the segmented MSCT data. Segmentation of CT-like 3DRA is more challenging than MSCT data due to the poorer

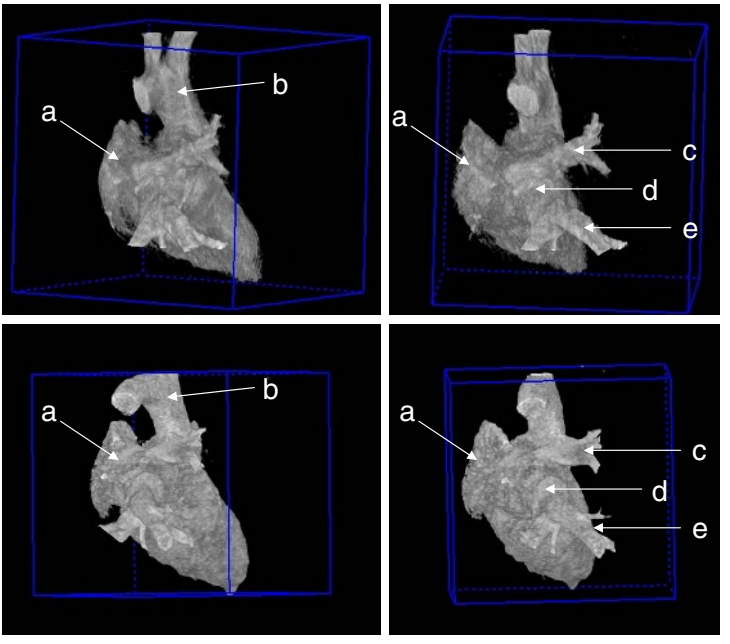

Fig. 3. Upper row shows volume renderings of a CT-like 3DRA reconstruction from a porcine study (posterior view orientation). (a) depicts the left atrial appendage, (b) is the aortic arc, (c) shows the right superior PV, (d) shows the LA and (e) indicates the right inferior PV. Lower row displays renderings from pre-operative MSCT imaging.

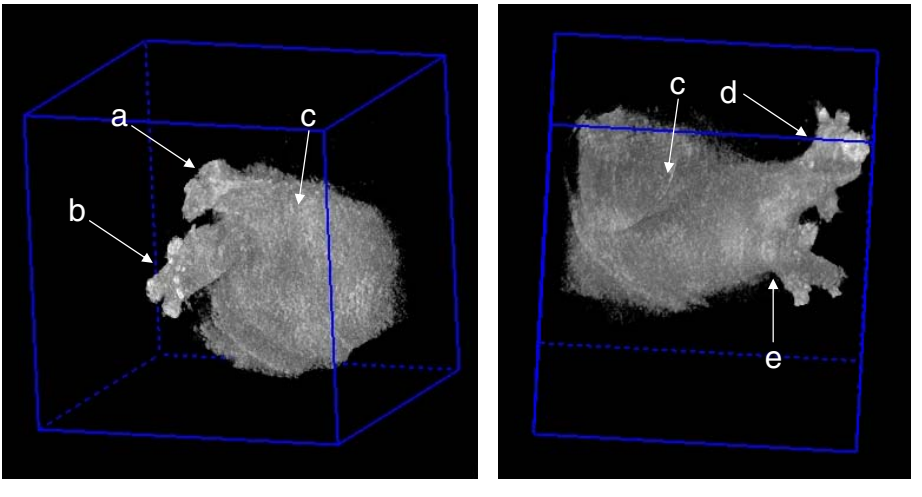

Fig. 4. On the left, a posterior volume rendering of the selective left pulmonary artery injection is shown. (a) reflects the left superior PV, (b) points at the left inferior PV and (c) shows a part of the LA. Right image illustrates the selective right pulmonary artery injection. (c) shows a part of the LA, (d) shows the right superior PV and (e) shows the right inferior PV.

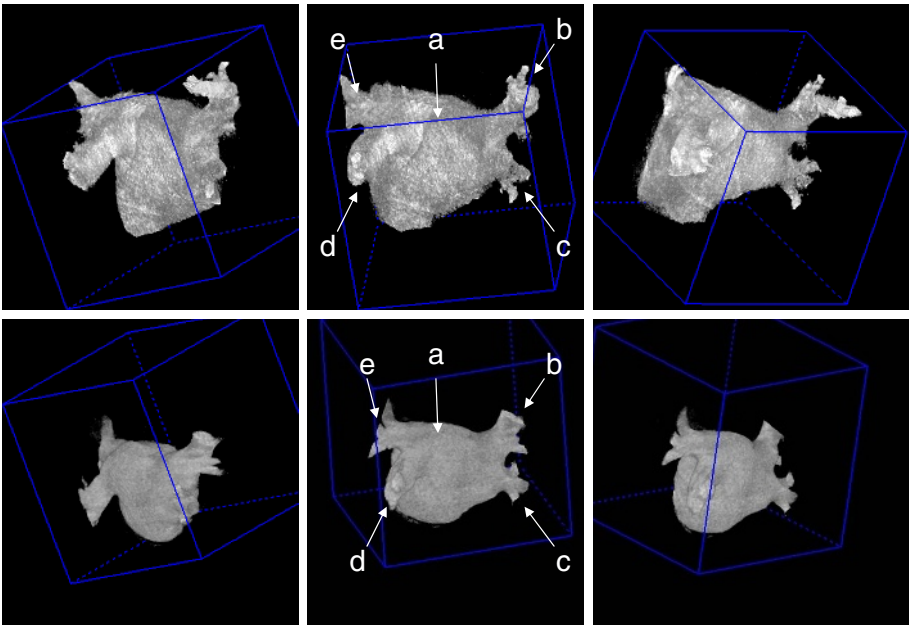

Fig. 5. Top row shows volume renderings from the reconstructed 3DRA run. (a) indicates the LA structure, (b) shows the right superior PV, (c) depicts the right inferior PV, (d) shows the left inferior PV and (e) indicates the left superior PV. Lower row displays renderings from the corresponding pre-operative CT data.

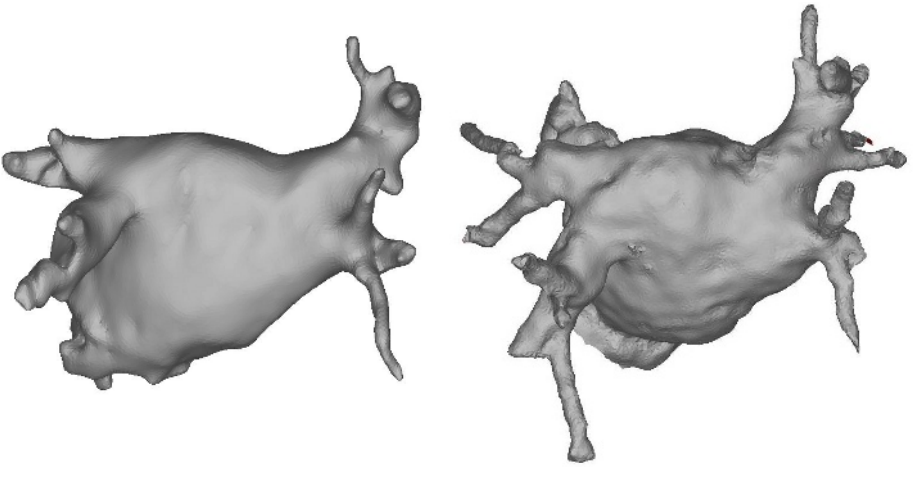

Fig. 6. Left image shows a view of the LAPV surface model, segmented from the fused 3DRA data set. Right image shows a segmentation from MSCT.

signal-to-noise characteristics, contrast levels, and artifacts from catheters and motion within the imaging field.

4 Conclusion and Future Work

We have presented a method for intra-operative volumetric imaging data of the LAPV anatomy that reflects the patient's anatomy at the moment of the intervention. This technique has the potential to be used during clinical AFib ablation procedures for improved 3D interventional navigation and may eliminate the need for pre-interventional volume imaging. Comparisons with pre-operative CT data reveal good qualitative correspondence. Compared with MSCT, a smaller X-ray dose is required to obtain useful images of the LAPV anatomy, reducing the overall radiation exposure to the patient.

Our future work will focus on a quantitative comparison with pre-operative volumetric images. Further optimization for automated acquisition protocol timing to account for pulmonary transit times will be performed. Finally, improvements in segmentation tools for automated surface model extraction will be explored.

References

[1] Haissaguerre, M., Jais, P., Shah, D.C., Takahashi, A., Hocini, M., Quiniou, G., Garrigue, S., Mouroux, A.L., Metayer, P.L., Clementy, J.: Spontaneous initiation of atrial fibrillation by ectopic beats originating in the pulmonary veins. New England Journal of Medicine **339** (1998) 659 – 666

[2] Pappone, C., Oreto, G., Rosanio, S., et al.: Atrial electroanatomic remodeling after circumferential radiogrequency pulmonary vein ablation: efficacy of an anatomic approach in a large cohort of patients with atrial fibrilation. Circulation **104** (2001) 2539 – 2544

[3] Reddy, V.Y., Malchano, Z.J., Holmvang, G., Schmidt, E.J., dAvila, A., Houghtaling, C., Chan, R.C., Ruskin, J.N.: Integration of cardiac magnetic resonance imaging with three-dimensional electroanatomic mapping to guide left ventricular catheter manipulation. Journal of the American College of Cardiology **44**(1) (2004) 2202 – 2213

[4] Mikaelian, B.J., Malchano, Z.J., Neuzil, P., Weichet, J., Doshi, S.K., Ruskin, J.N., Reddy, V.Y.: Integration of three-dimensional cardiac computed tomography images with real-time electroanatomic mapping to guide catheter ablation of atrial fibrillation. Circulation **112** (2005) 35 – 36

[5] Feldkamp, L.A., Davis, L.C., Kress, J.W.: Practical cone-beam algorithm. Journal of the Optical Society of America **A6** (1984) 612 – 619

[6] Movassaghi, B.: Ph.D. thesis on 3D rotational X-ray coronary angiography. Utrecht University, ISBN:90-393-05048 (2004)

[7] Lorensen, W.E., Cline, H.E.: Marching cubes: A high resolution 3d surface construction algorithm. In: SIGGRAPH '87: Proceedings of the 14th annual conference on Computer graphics and interactive techniques, New York, NY, USA, ACM Press (1987) 163–169